Supplementary Information

Rational incorporation of covalent organic framework/carbon nanotube (COF/CNT) composites for electrochemical aptasensing of ultra-trace atrazine

Qian-Qian Zhu,[a] Hong-Kai Li,[a] Xiao-Long Sun,[a] Zhang-Ye Han,[a] Jianchao Sun,[b] and Hongming He*[a]

[a] *Tianjin Key Laboratory of Structure and Performance for Functional Molecules, College of Chemistry, Tianjin Normal University, Tianjin 300387, China*

[b] *School of Environment and Material Engineering, Yantai University, Yantai, Shandong 264005, China*

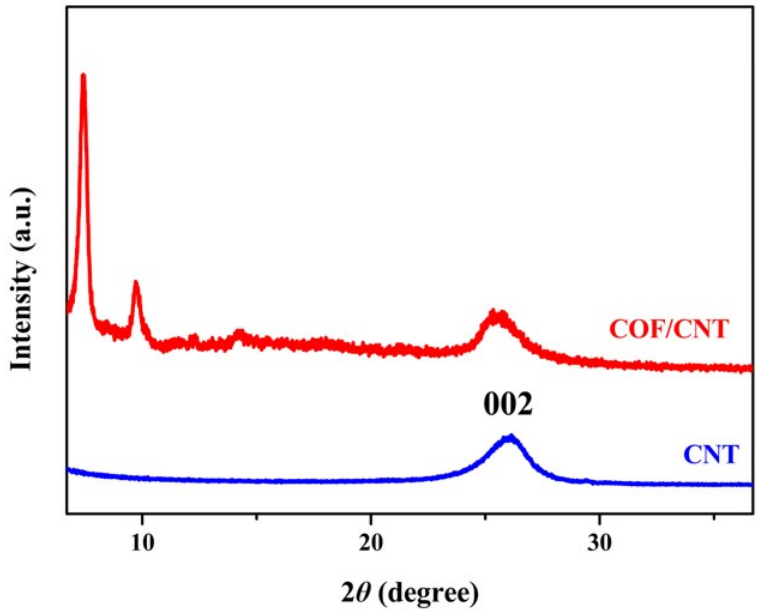

Figure S1. The PXRD patterns of COF/CNT and CNT.

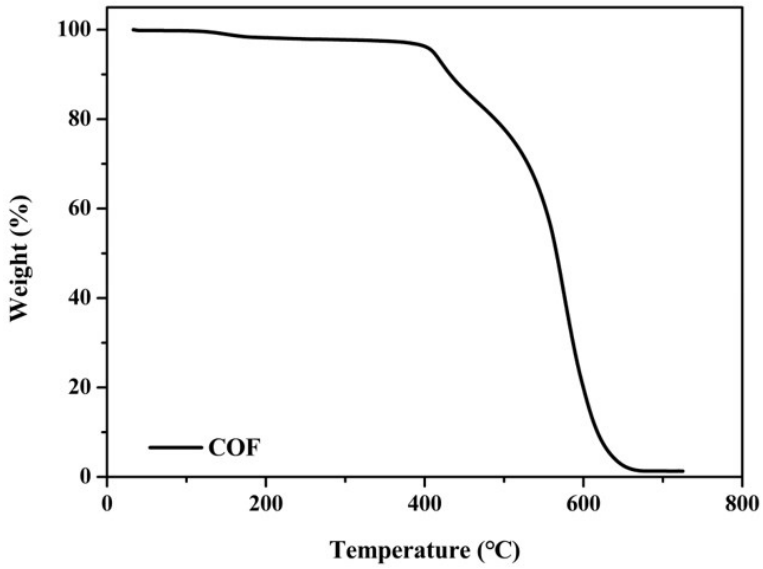

Figure S2. The TG curve of COF.

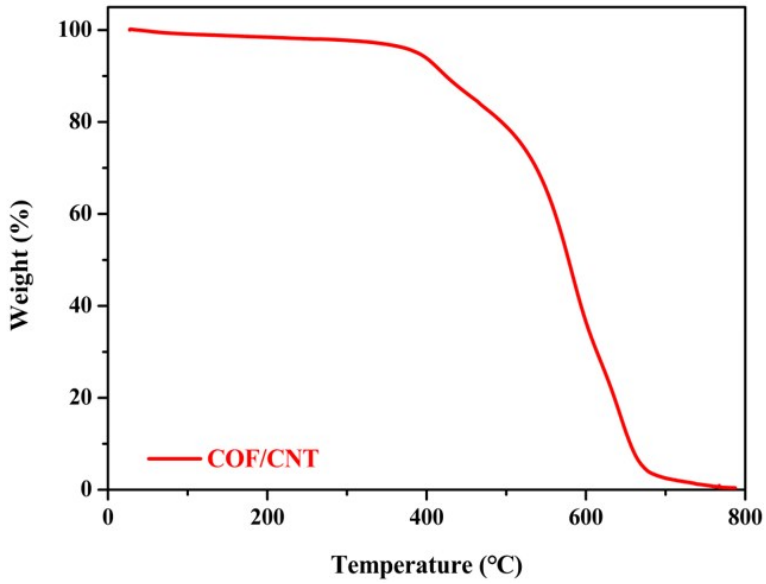

Figure S3. The TG curve of COF/CNT.

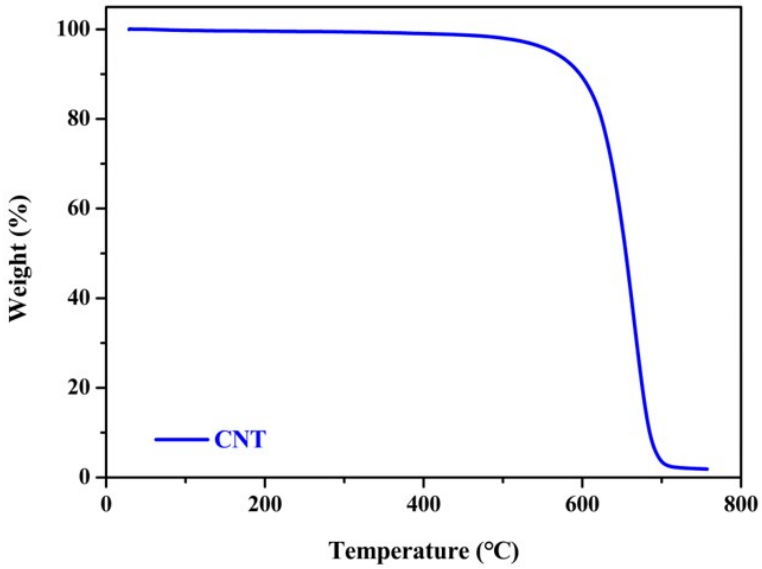

Figure S4. The TG curve of CNT.

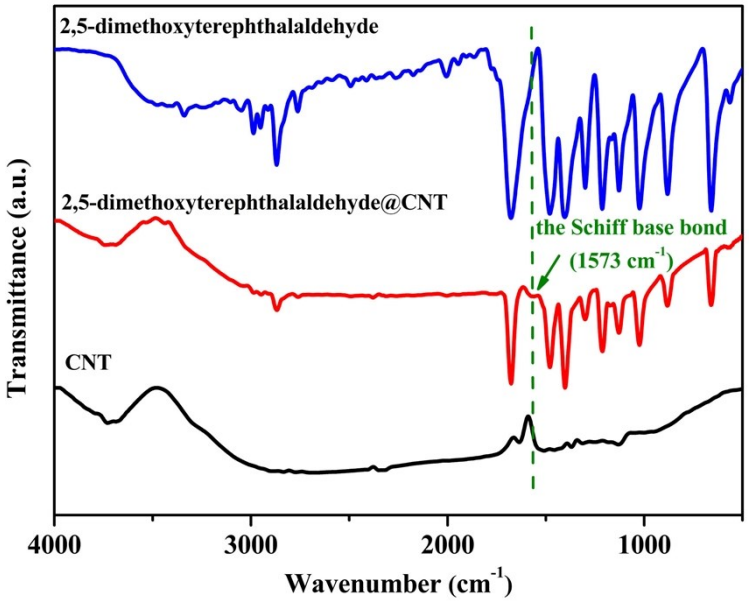

Figure S5. The FT-IR spectra.

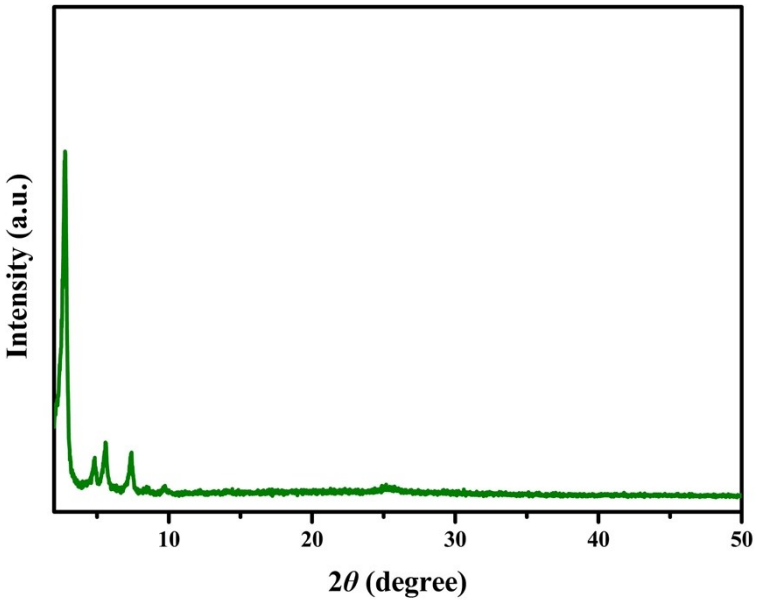

Figure S6. The PXRD pattern of activated sample.

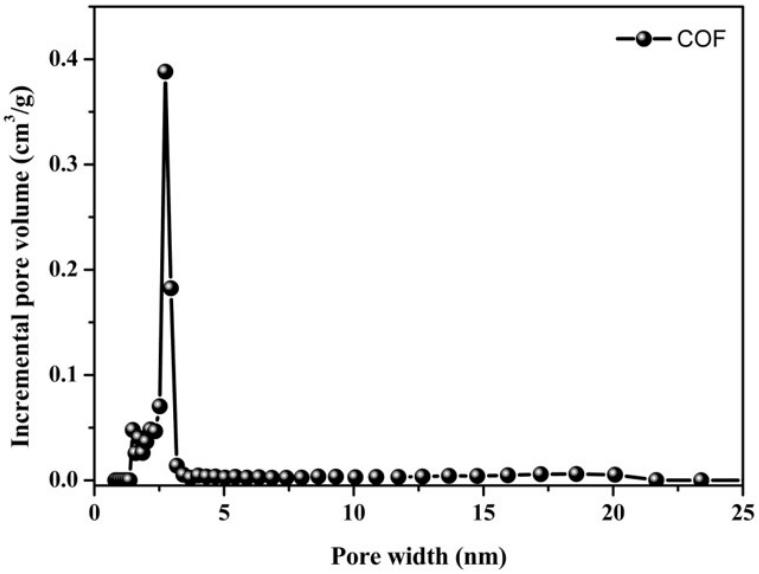

Figure S7. The pore size distribution of COF.

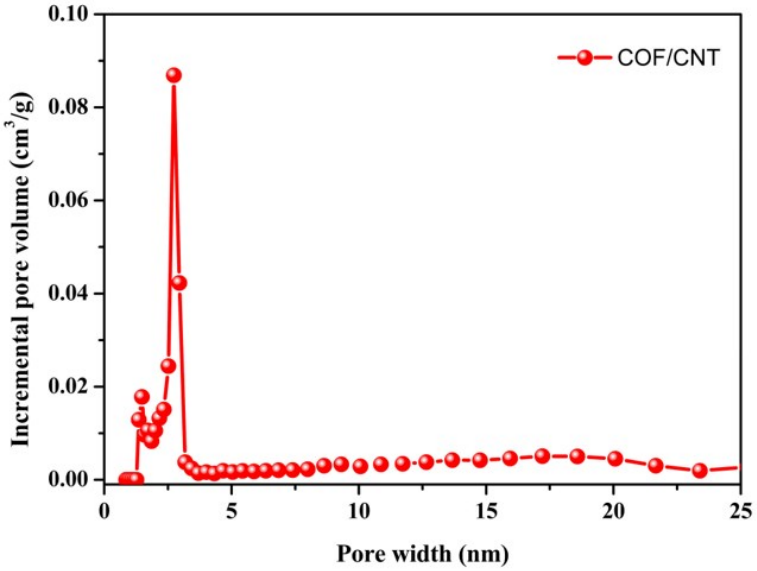

Figure S8. The pore size distribution of COF/CNT.

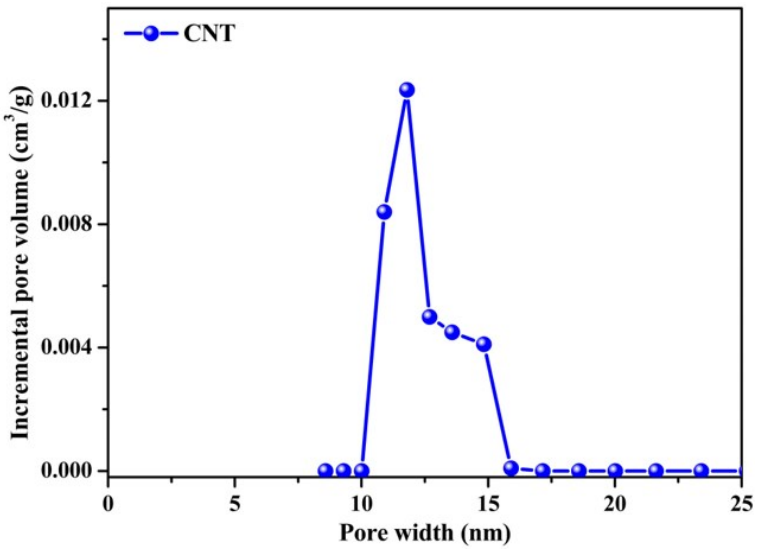

Figure S9. The pore size distribution of CNT.

Figure S10. The TEM images of CNT.

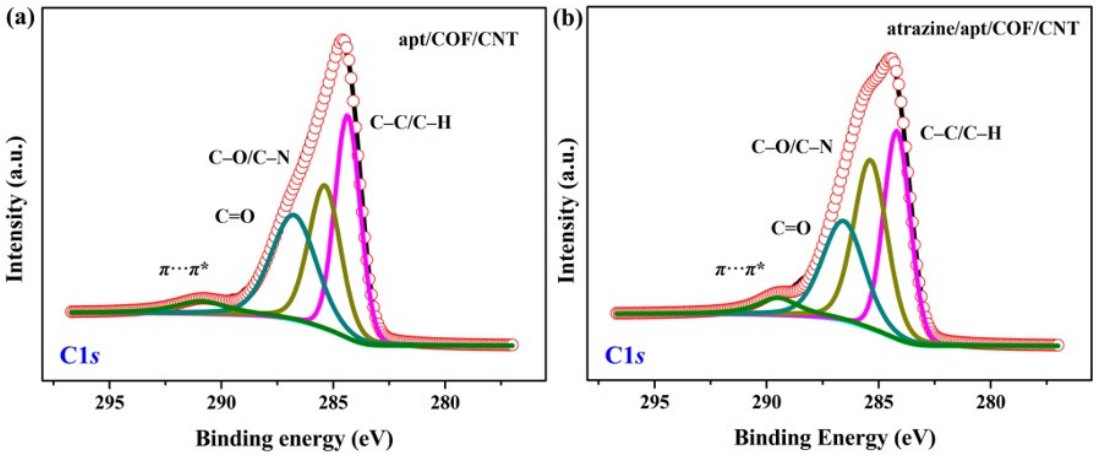

Figure S11. The high-resolution XPS spectra of C 1*s* in (a) apt/COF/CNT and (b) atrazine/apt/COF/CNT.

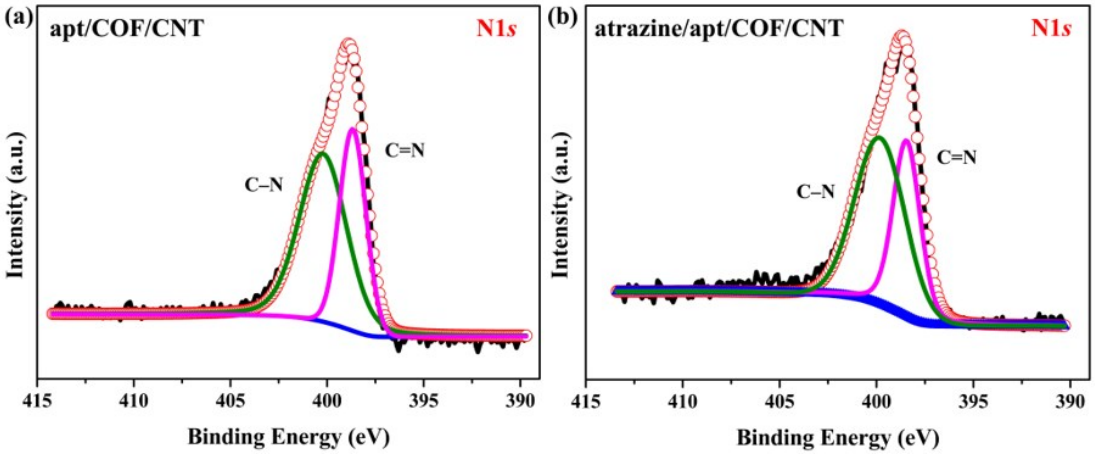

Figure S12. The high-resolution XPS spectra of N 1*s* in (a) apt/COF/CNT and (b) atrazine/apt/COF/CNT.

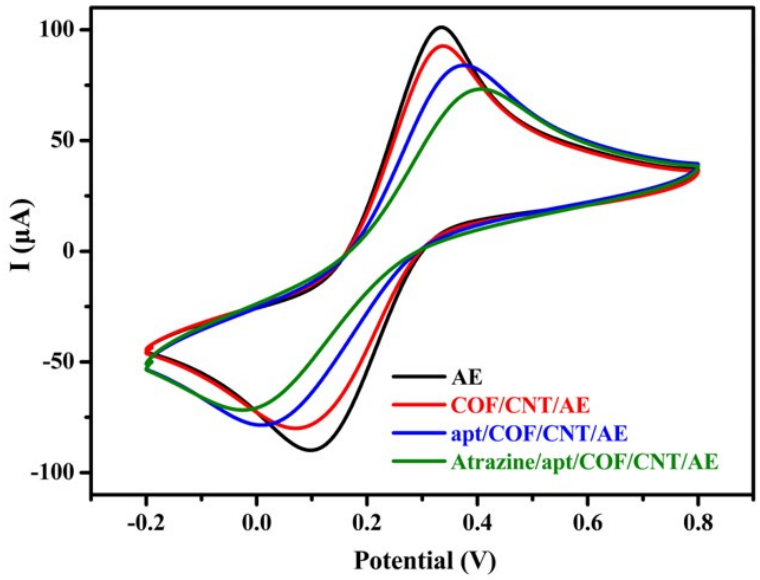

Figure S13. CV curves of different modified electrodes for the COF/CNT-based aptasensor.

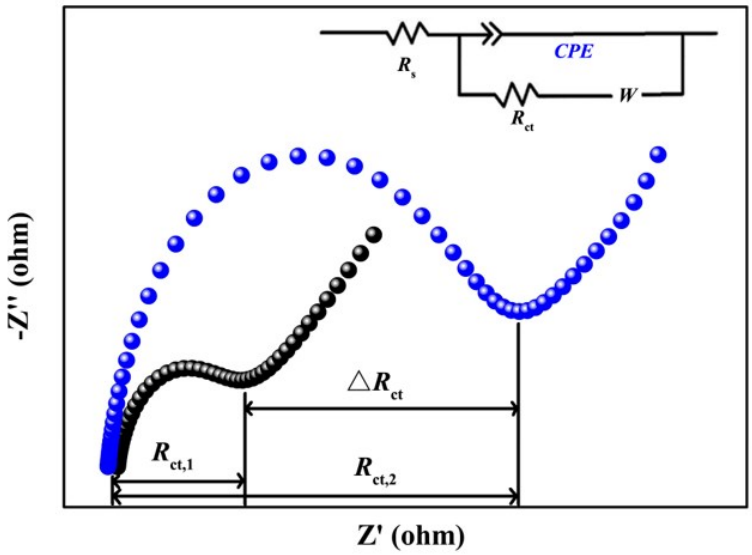

Figure S14. EIS Nyquist plots with the equivalent circuit.

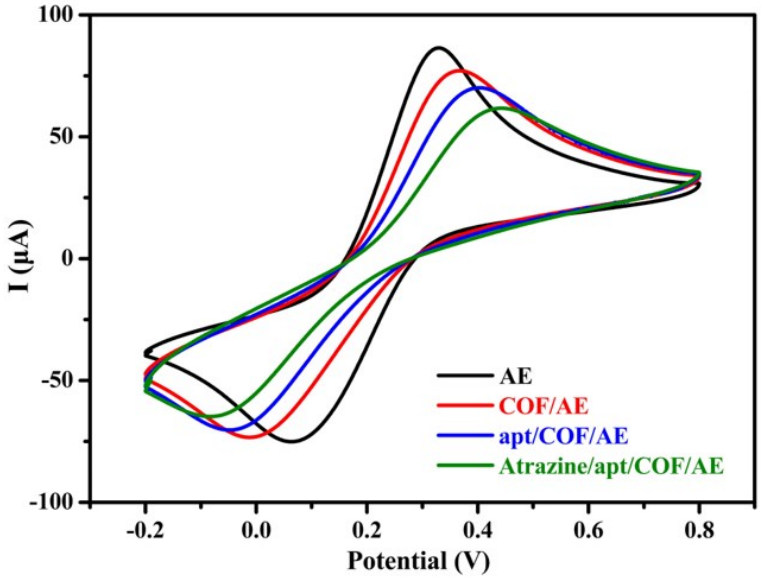

Figure S15. CV curves of different modified electrodes for the COF-based aptasensor.

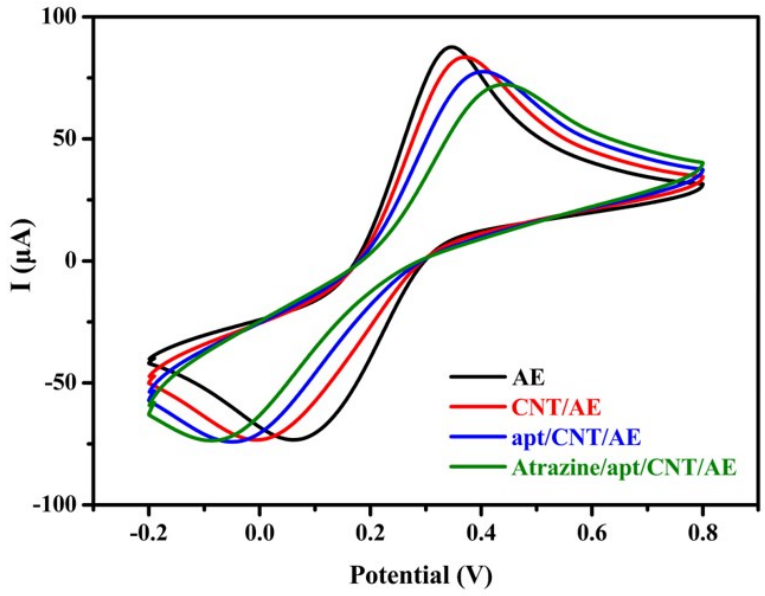

Figure S16. CV curves of different modified electrodes for the CNT-based aptasensor.